



Supplement of

Examining the effects of anthropogenic emissions on isoprene-derived secondary organic aerosol formation during the 2013 Southern Oxidant and Aerosol Study (SOAS) at the Look Rock, Tennessee, ground site

S. H. Budisulistiorini et al.

Correspondence to: J. D. Surratt (surratt@unc.edu)

A. Ambient PM₁ and Collocated Measurements

Table S1. Collocated gas- and particle-phase measurements at LRK site.

Compound	Instrument	Analysis Method	Reporting Frequency
SO ₂	Thermo Scientific 43i TLE	Pulsed fluorescence	1 hr
CO	Thermo Scientific 48i TLE	NDIR-GFC	1 hr
NO	Thermo Scientific 42c	Chemiluminescence	1 hr
NO _y	Thermo Scientific 42c	Chem./Mo converter	1 hr
NO ₂	API 200EU	Chem./photolytic conv.	1 hr
BC	Magee AE 22	Optical absorption	1 hr
SO ₄	Thermo Scientific 5020	Thermal/fluorescence	1 hr
PM _{2.5}	Met One BAM-1020	Beta attenuation	1 hr
PM ₁₀	Met One BAM-1020	Beta attenuation	1 hr
O ₃ ^a	Thermo Scientific 49i	UV absorption	1 hr

^aOzone is measured at National Park Service shelter next to LRK shelter

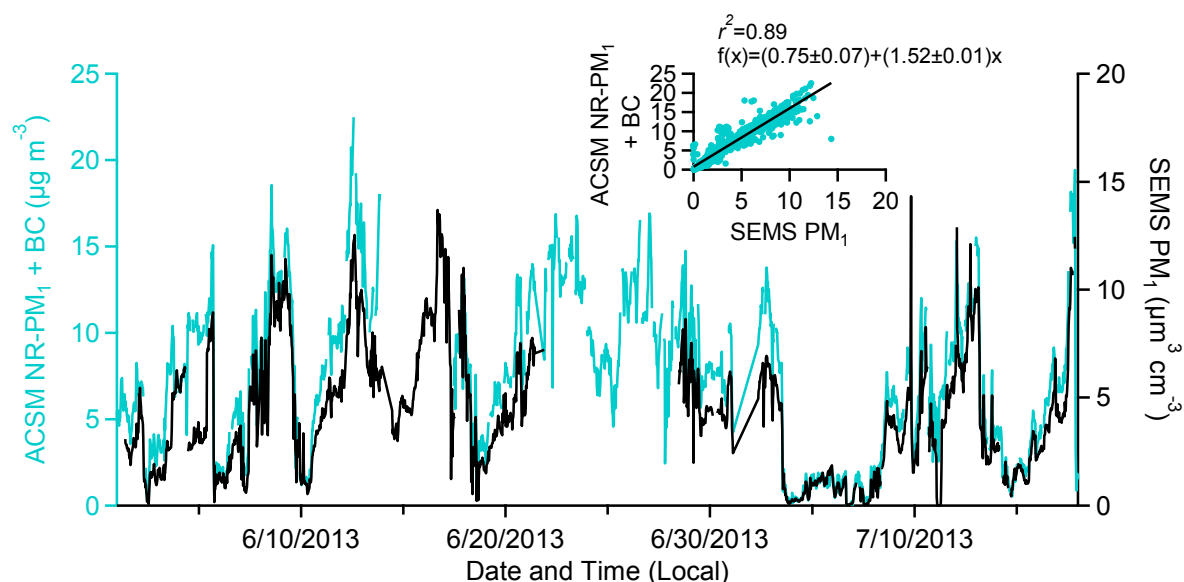


Figure S1. Comparison of PM₁ mass concentration from ACSM and black carbon measurements with PM₁ volume concentration from SEMS suggests a strong correlation. Slope shown in insert suggests an estimated aerosol density of 1.52 g cm⁻³.

B. PMF Analysis

Table S2. Summary of PMF solutions obtained for 2013 SOAS campaign dataset.

# Factors	FPEAK	SEED	$Q/Q_{expected}$	Solution Description
1	0	0	0.27262	One-factor (OOA) resulted in large residuals at some time periods and m/z 's.
2	0	0	0.23717	Two-factor (IEPOX-OA and LV-OOA) is significantly reduced residuals. LV-OOA factor time trends and mass spectrum seem to be a mixture of less- and more-oxidized OA.
3	0	0	0.21338	Three-factor (IEPOX-OA, LV-OOA, and 91Fac) seems like an optimum solution. The 91Fac appears to share some similarities in time trend and mass spectrum to IEPOX-OA and LV-OOA but with a distinct m/z 91.
3	-0.2 to 0.2	0	0.2134-0.21447	In this range, factor MS and time series are changing suggesting possibility of optimum solution.
3	-0.09	0	0.2137	Optimum number of factors (IEPOX-OA, LV-OOA, and 91Fac) and FPEAK. All three factors have distinctive time trends and mass spectra, and compare well with independent particle and/or gaseous measurements, and reference MS from database and/or experiment in this study.
3	0	0-100 in steps of 5	0.21336-0.21353	For 3-factor, time trends and mass spectra are nearly identical at different starting points.
4 to 10	0	0	0.19965-0.16295	Q/Q_{exp} is reduced but OOA factor is split into more factors that do not compare well with reference MS.

Table S3. Correlation of PMF 2-, 3-, and 4-factor solutions at Fpeak 0 with collocated measurements and reference mass spectra.

	2-factor		3-factor			4-factor			
	Fac1	Fac2	Fac1	Fac2	Fac3	Fac1	Fac2	Fac3	Fac4
r_{TS}^2									
CO	0.41	0.33	0.37	0.44	0.28	0.37	0.45	0.34	0.29
NO _x (=NO+NO ₂)	0.02	0.01	0.03	0.01	0.02	0.03	0.01	0.00	0.05
NO _y	0.15	0.22	0.14	0.21	0.20	0.13	0.22	0.17	0.22
NO _z	0.15	0.22	0.14	0.21	0.21	0.13	0.21	0.17	0.23
O _x (=NO ₂ +O ₃)	0.18	0.21	0.15	0.30	0.13	0.14	0.32	0.16	0.16
SO4	0.37	0.16	0.35	0.31	0.14	0.35	0.33	0.19	0.17

	2-factor		3-factor			4-factor			
	Fac1	Fac2	Fac1	Fac2	Fac3	Fac1	Fac2	Fac3	Fac4
ACSM SO ₄	0.62	0.34	0.59	0.53	0.31	0.59	0.55	0.39	0.33
ACSM NO ₃	0.75	0.73	0.72	0.80	0.70	0.70	0.79	0.74	0.68
ACSM NH ₄	0.61	0.41	0.57	0.59	0.36	0.57	0.61	0.44	0.37
r^2_{MS}									
HOA	0.11	0.05	0.17	0.03	0.57	0.18	0.02	0.35	0.29
LV-OOA	0.97	0.97	0.83	0.93	0.32	0.80	0.91	0.67	0.52
SV-OOA	0.55	0.41	0.64	0.32	0.88	0.64	0.28	0.91	0.44
BBOA	0.46	0.28	0.64	0.20	0.69	0.66	0.17	0.69	0.34
82Fac	0.89	0.71	0.94	0.60	0.47	0.94	0.56	0.68	0.38
91Fac	0.54	0.42	0.60	0.32	0.80	0.58	0.27	0.67	0.69
IEPOX-OA	0.81	0.65	0.89	0.56	0.53	0.89	0.52	0.84	0.33
Lab IEPOX SOA	0.55	0.32	0.80	0.24	0.38	0.83	0.21	0.53	0.19

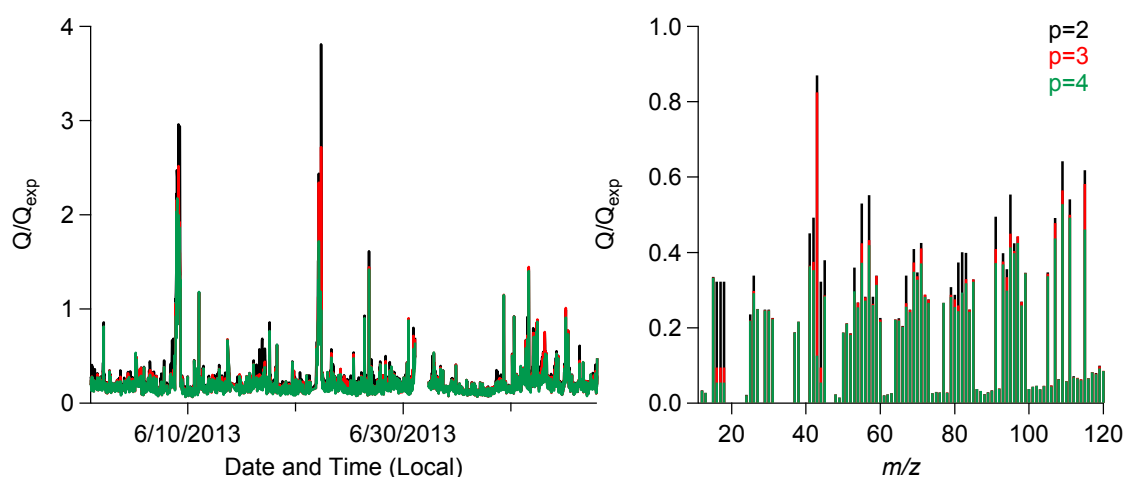


Figure S2. Time series and mass spectra of Q/Q_{exp} for 2-, 3-, and 4-factor solutions are used to determine the optimum number of factor in PMF analysis. The 3-factor solution time series and mass spectra of Q/Q_{exp} suggest that adding the third factor reduces Q/Q_{exp} substantially. The 4-factor solution does not significantly reduce time series and mass spectrum of Q/Q_{exp} compared to those of 3-factor solution.

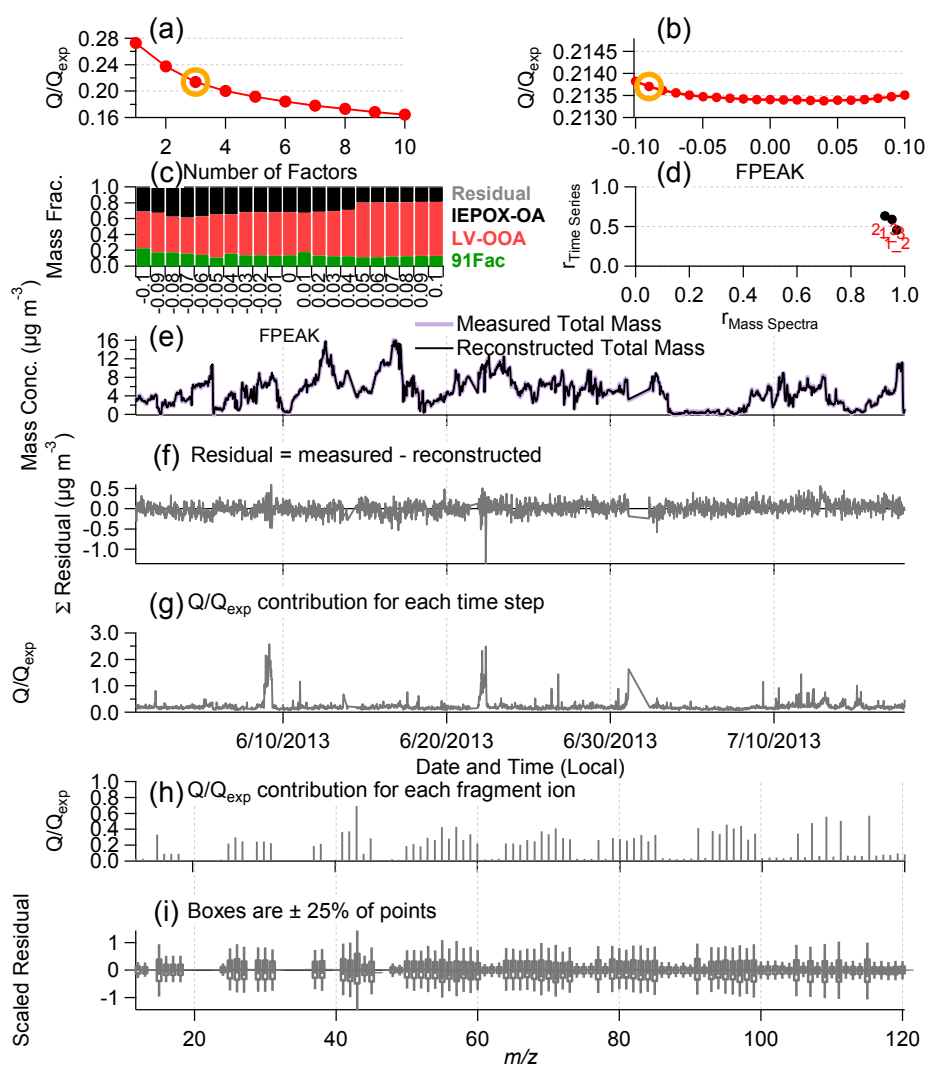


Figure S3. Diagnostic plots for PMF analysis of 2013 SOAS campaign dataset: (a) Q/Q_{exp} as a function of number of factors (p), (b) Q/Q_{exp} as a function of FPEAK selected for the chosen number of factors, (c) fractional contribution of OA factors for each FPEAK, (d) correlation among PMF factors based on factor TS and MS, (e) TS of the measured OA mass and the reconstructed OA mass, (f) variation of the residual of the fit, Q/Q_{exp} for each point in time (g) and for each m/z (h), and the box and whisker plot of the scaled residuals for each m/z .

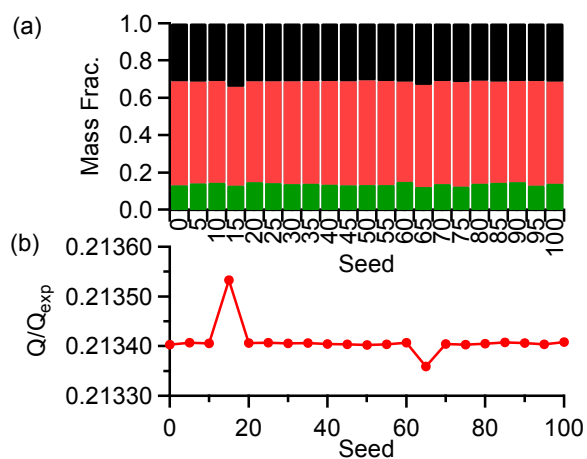


Figure S4. Diagnostic plots for seed analysis of PMF three factor solution: (a) fractional contribution of OA factors for each seed, and (b) Q/Q_{exp} as a function of seed selected for the chosen number of factors. Changes in mass fraction contribution of each factor are negligible ($< 1\%$) over seed range. Similarly, Q/Q_{exp} values at different seed are nearly identical with very small changes ($< 1\%$).

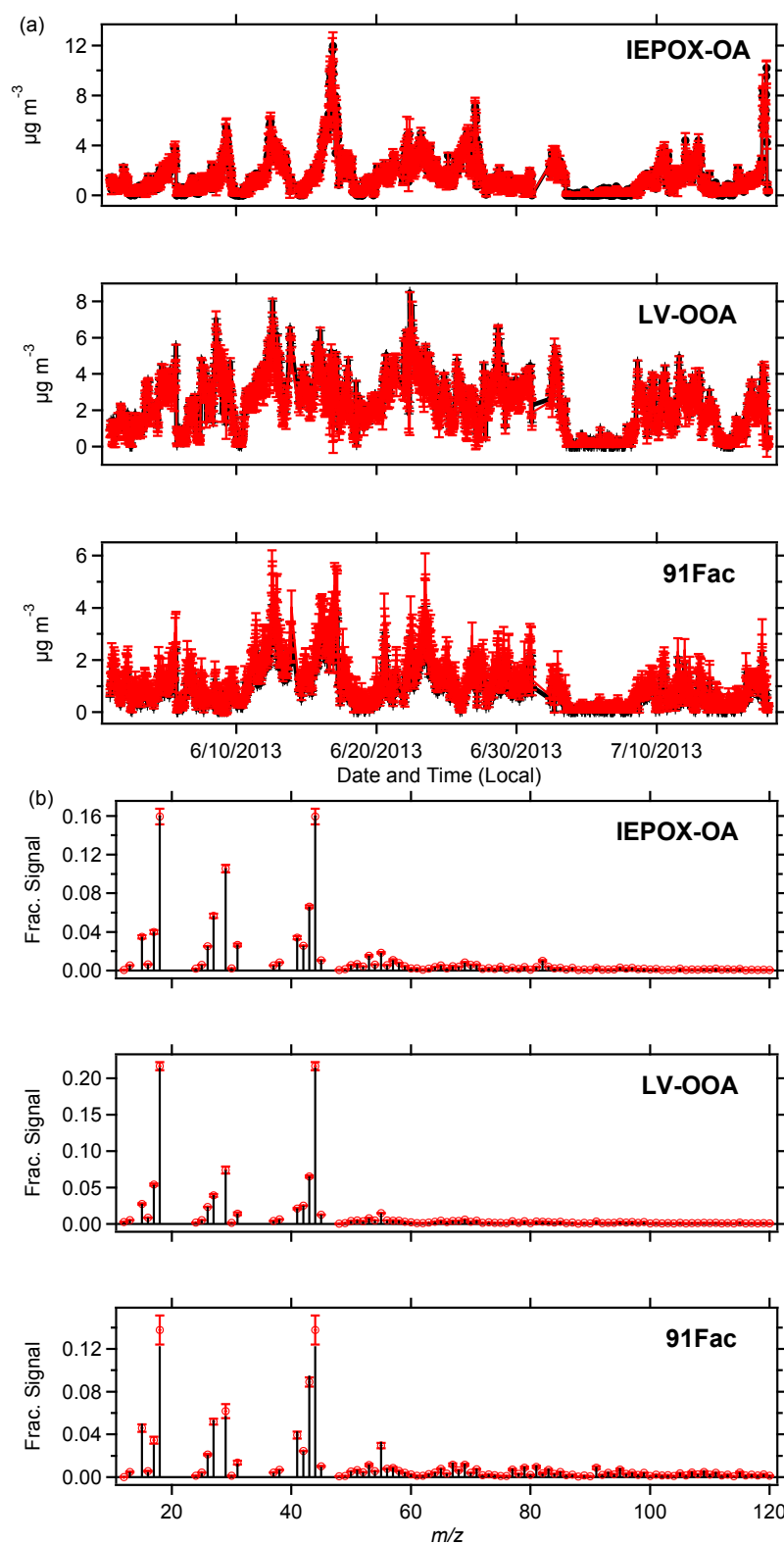


Figure S5. Results from bootstrapping analysis of the three factor solution of the 2013 SOAS campaign dataset. Average (a) time series and (b) mass spectra are shown in black with 1- σ error bars in red. All four factors show some uncertainty in their mass spectra and time series, which are nonetheless small compared to the general factor profile and contribution.

C. Filter Sampling Methods and Analysis

FLEXPART Model

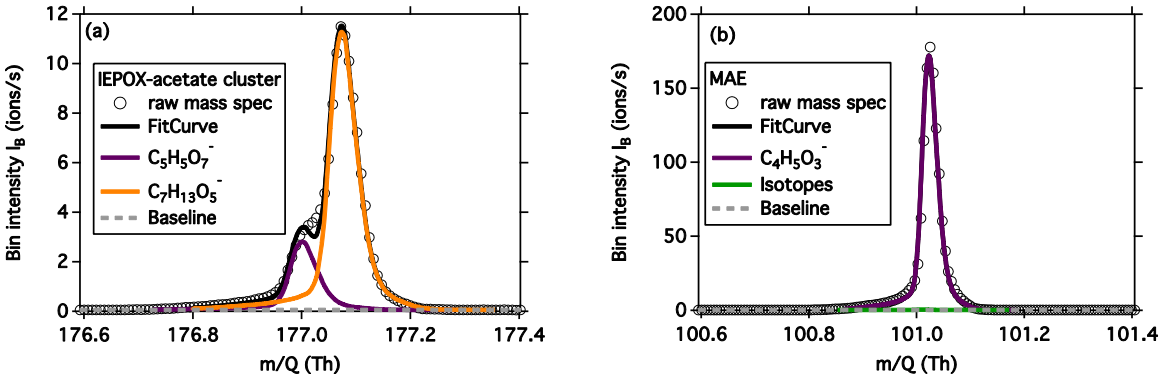
The intensive filter sampling periods were selected on the basis of the FLEXPART Lagrangian particle dispersion model v. 9.02 (Stohl et al., 2005), driven by analytical data (every 6 hours) and 3 hour forecasts of the Global Forecast System (GFS) of the National Centers for Environmental Prediction (NCEP). Back-trajectory calculations were conducted on a 0.1 x 0.1 degree grid by releasing 10000 air parcels every 3 hours at each SAS field site and following parcels back in time for 72 hours. The resulting 3-hour surface residence time fields (concentration of parcels at a given time between 0 and 100 m above ground) were convolved with emission inventories and then spatially integrated to estimate total emissions injected into the air parcel during each 3-hour interval. This allowed estimation of (1) total emissions load of an air mass sampled at LRK (as well as the other ground sites), (2) the mixture of different emission source types (mobile, biogenic VOCs, biomass burning, etc.), and (3) the age (and hence amount of chemical processing) emissions experienced prior to arrival at LRK. NO_x and SO₂ concentrations were estimated from the National Emission Inventory (NEI), biomass burning emissions from the Fire Inventory from NCAR (FINN, Wiedinmyer et al., 2011) and biogenic VOC emissions were based on results of a MOZART global model (Emmons et al., 2010) simulation using the Model of Emissions of Gases and Aerosols from Nature (MEGAN, Guenther et al., 2006).

1 **Filter Analysis**

2 **Table S4.** Temperature program and purge gas type used in OC/EC analysis of particle-laden
3 filter punches.

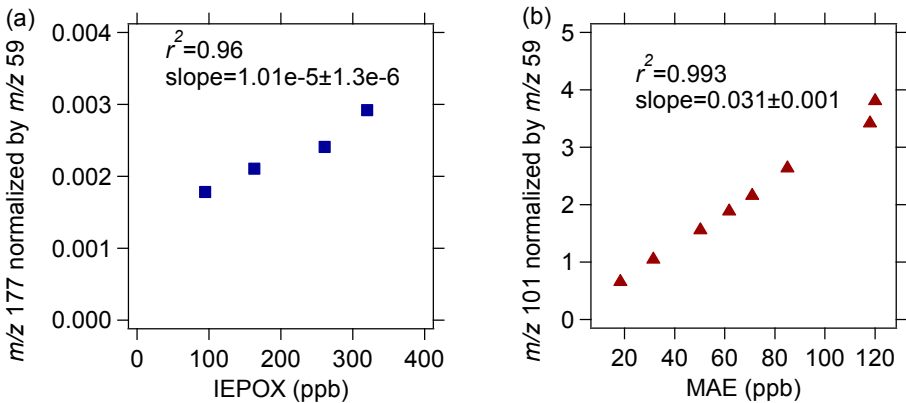
Step	Gas	Hold time (s)	Temperature (°C)
1	He	60	310
2	He	60	480
3	He	60	615
4	He	90	900
5	He	30	Oven off
6	He	8	550
7	He/O ₂	35	600
8	He/O ₂	45	675
9	He/O ₂	45	750
10	He/O ₂	45	825
11	He/O ₂	120	920

4



5 **Figure S6.** Typical high-resolution fitting of (a) IEPOX as an acetate cluster, and (b) MAE as
6 a deprotonated ion from HR-ToF-CIMS measurement at LRK site.

7



8 **Figure S7.** Calibration factors of (a) IEPOX and (b) MAE from HR-ToF-CIMS with acetate
9 ion chemistry.

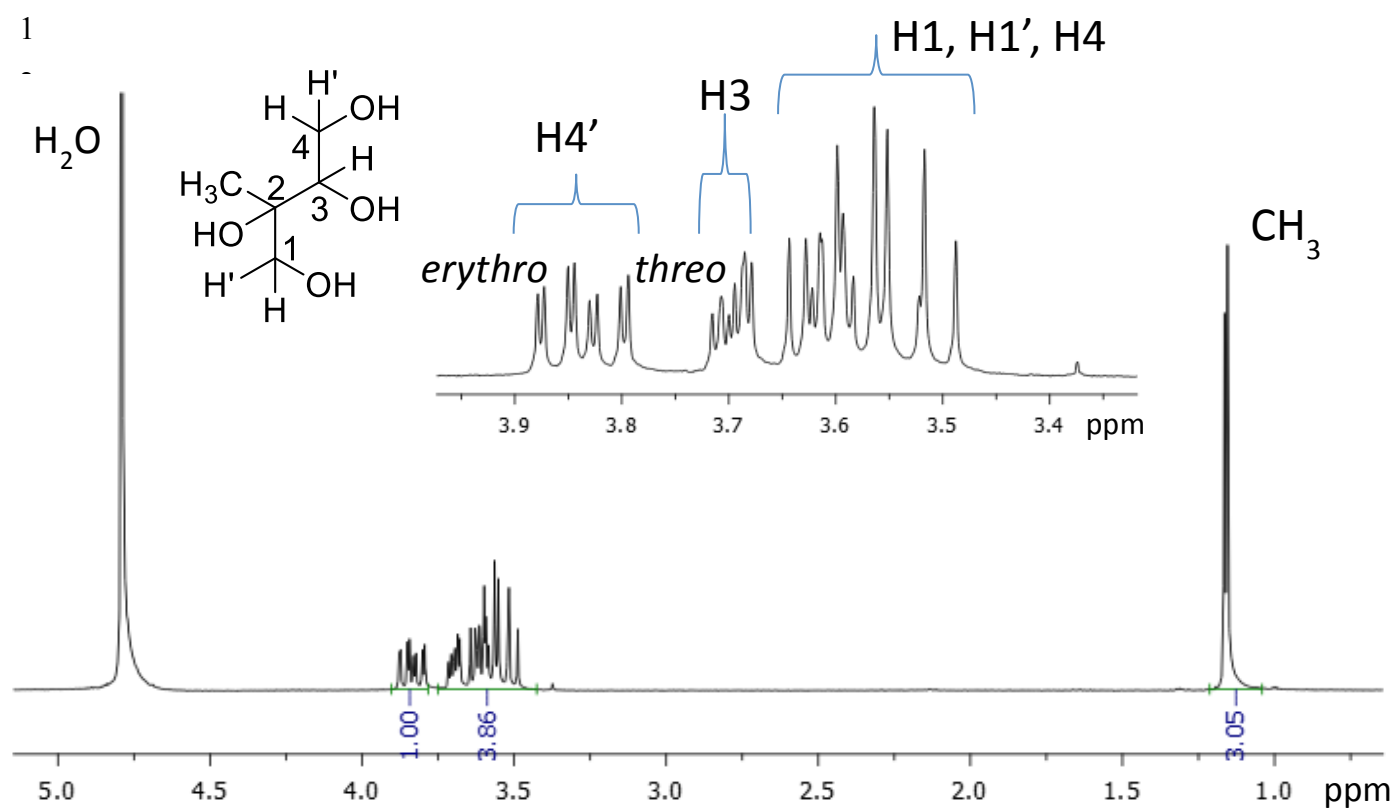


Figure S8. ^1H NMR spectrum (D_2O , 400 MHz) of 2-C-methylerythritol and 2-C-methylthreitol mixture.

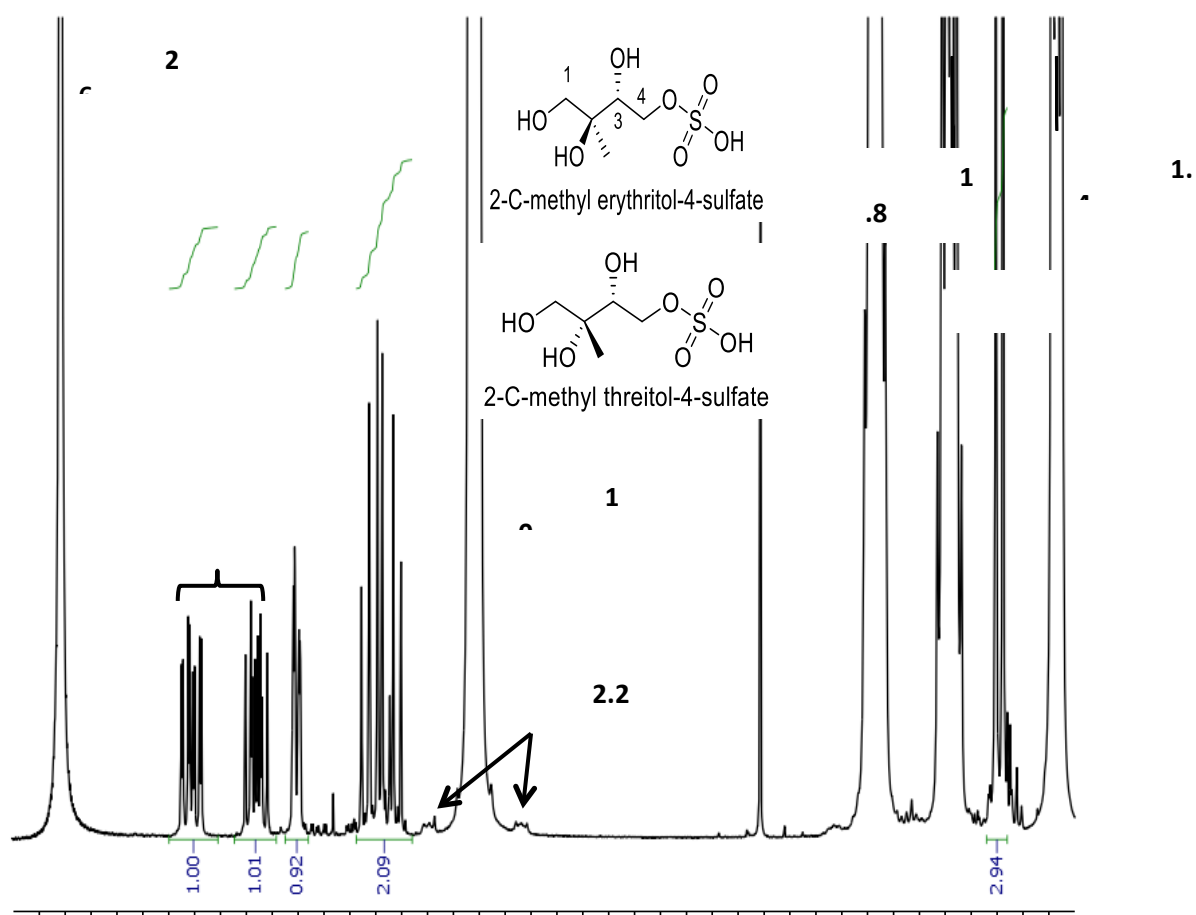


Figure S9. ^1H NMR spectrum (D_2O , 400 MHz) of 2-C-methyltetrol sulfate ester mixture.

D. Gas- and Particle-phase Analysis

Table S5. Correlation of PMF Factors with collocated measurements and reference mass spectra.

	IEPOX-OA	LV-OOA	91Fac
<i>r² Time Series</i>			
CO	0.29	0.38	0.18
NO _x (=NO+NO ₂)	0.03	0.00	0.03
NO _y	0.09	0.19	0.16
NO _z	0.08	0.16	0.15
O _x (=NO ₂ +O ₃)	0.07	0.36	0.06
SO ₄	0.31	0.23	0.07
ACSM SO ₄	0.58	0.39	0.18
ACSM NO ₃	0.55	0.62	0.55
ACSM NH ₄	0.47	0.48	0.23
CIMS MAE	0.27	0.30	0.33
CIMS IEPOX	0.24	0.31	0.37
PTR-MS Isoprene	0.01	0.08	0.05
PTR-MS MVK+MACR	0.36	0.37	0.47
PTR-MS Acetonitrile	0.12	0.09	0.07
PTR-MS Monoterpenes	0.00	0.02	0.01
LWC	0.00	0.06	0.00
pH	0.05	0.08	0.02
WSOC	0.37	0.28	0.27
<i>r² Mass Spectra</i>			
HOA ^a	0.11	0.05	0.24
LV-OOA ^a	0.97	0.97	0.92
SV-OOA ^a	0.55	0.41	0.75
BBOA ^a	0.46	0.28	0.56
82Fac ^b	0.89	0.71	0.82
91Fac ^b	0.54	0.42	0.75
IEPOX-OA ^c	0.81	0.65	0.83
Lab IEPOX SOA ^c	0.55	0.32	0.49

References: (a) Ng et al. (2011), (b) Robinson et al. (2011), and (c) Budisulistiorini et al. (2013)

Table S6. Correlation of isoprene-derived SOA tracers measured by GC/EI-MS and UPLC/DAD-ESI-HR-Q-TOFMS with collocated measurements.

r^2	MeTHF	MeTetrol	Triol	2-MG	IEPOXOS	IEPOXOSdimer	MAEOS
CO	0.07	0.34	0.29	0.45	0.36	0.13	0.26
NO _x (=NO+NO ₂)	0.03	0.00	0.01	0.03	0.00	0.04	0.00
NO _y	0.16	0.11	0.12	0.38	0.13	0.02	0.22
NO _z	0.29	0.17	0.23	0.35	0.25	0.10	0.35
O _x (=NO ₂ +O ₃)	0.05	0.01	0.01	0.00	0.04	0.02	0.05
SO ₄	0.06	0.36	0.31	0.35	0.34	0.14	0.28
ACSM SO ₄	0.09	0.36	0.31	0.31	0.39	0.24	0.35
ACSM NO ₃	0.17	0.41	0.38	0.46	0.42	0.32	0.44
ACSM NH ₄	0.07	0.32	0.27	0.32	0.34	0.20	0.34
CIMS MAE	0.45	0.26	0.33	0.37	0.32	0.24	0.48
CIMS IEPOX	0.41	0.21	0.28	0.30	0.26	0.20	0.42
PTR-MS Isoprene	0.06	0.03	0.03	0.09	0.08	0.04	0.05
PTR-MS MVK+MACR	0.15	0.24	0.26	0.29	0.34	0.22	0.21
PTR-MS Acetonitrile	0.01	0.20	0.18	0.33	0.30	0.17	0.11
LWC	0.02	0.00	0.01	0.02	0.03	0.01	0.00
pH	0.07	0.05	0.06	0.06	0.11	0.07	0.05
WSOC	0.06	0.33	0.31	0.29	0.38	0.28	0.21

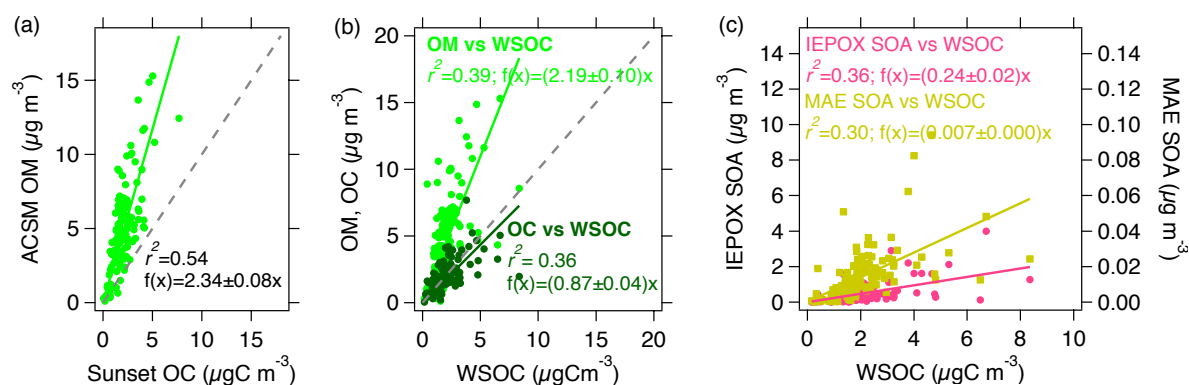


Figure S10. Comparisons of organic aerosol (OM) by ACSM with organic carbon (OC) by Sunset OC/EC (a) and water soluble organic carbon (WSOC) measurements (b). OM:OC ratio was estimated to be 2.34. Comparisons of WSOC with SOA tracers (c) indicate that IEPOX- and MAE-derived masses might explain 25% and 0.5% of the WSOC mass, respectively.

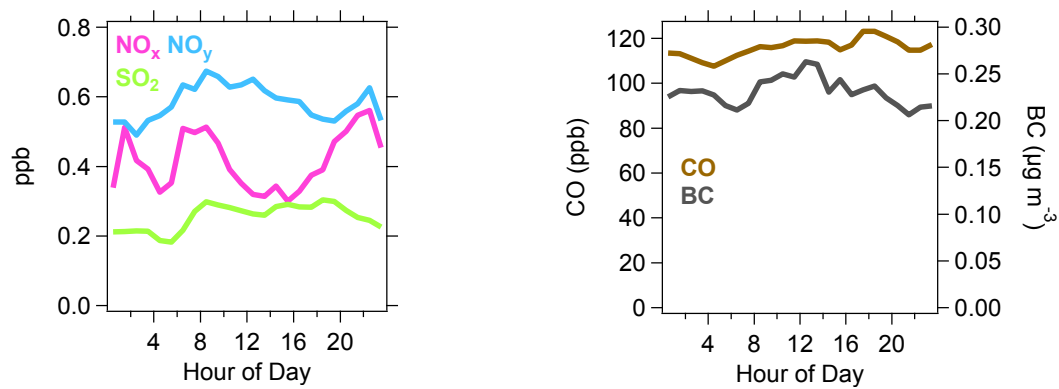
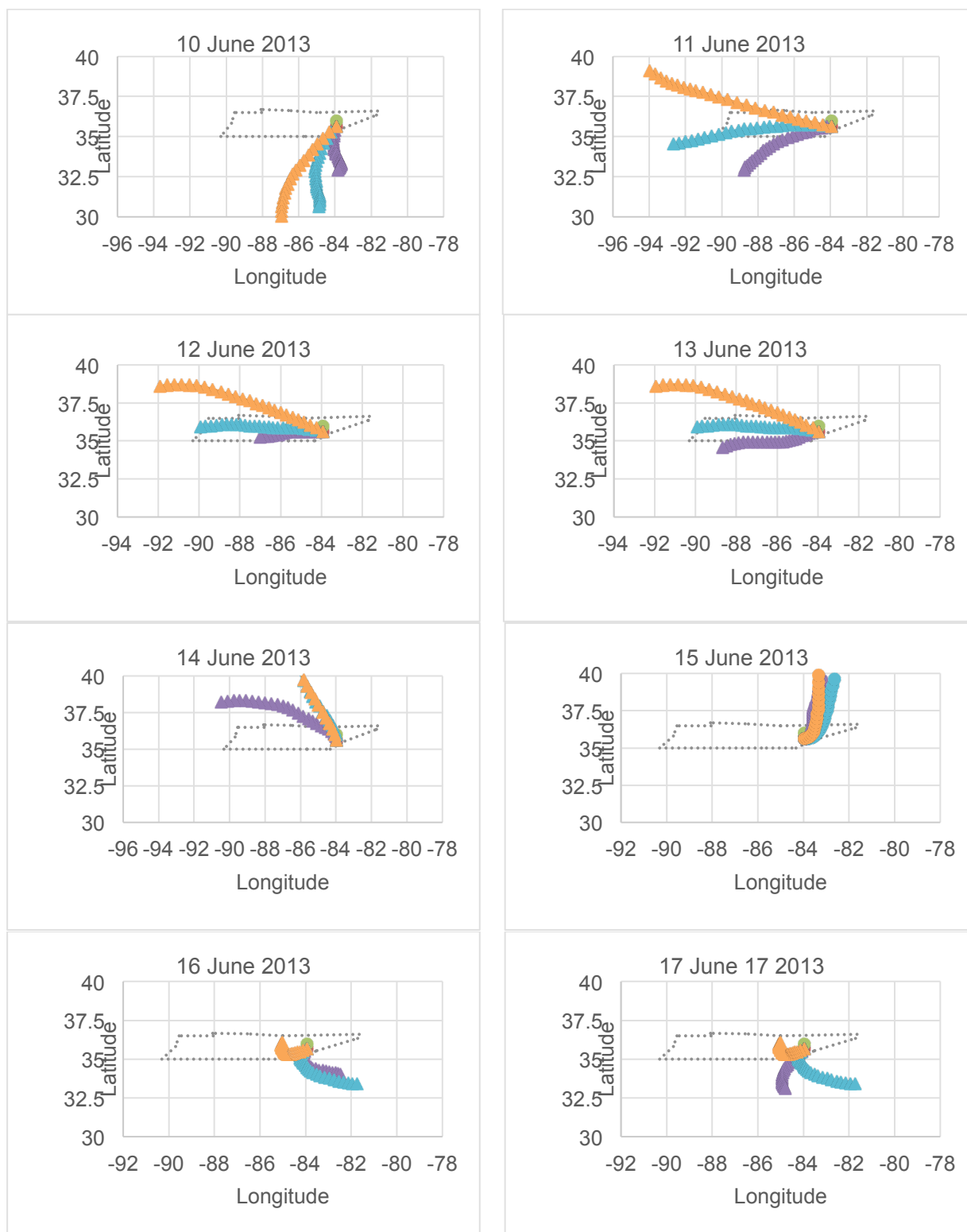


Figure S11. Diurnal variation of NO_x , NO_y , and SO_2 (left) and CO and BC (right). Overall, concentration of primary tracers (i.e., NO_x , SO_2 , CO, and BC) are small.

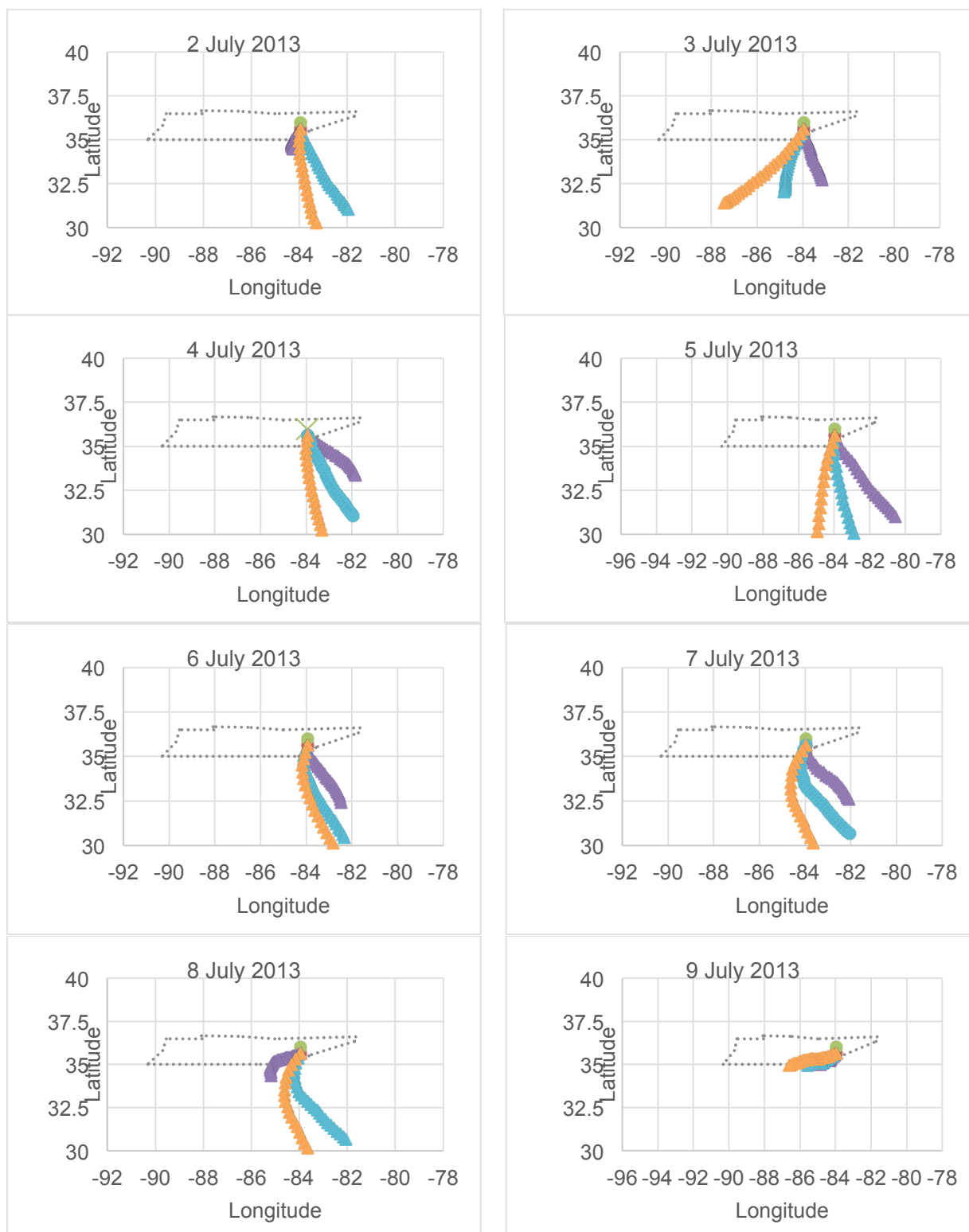
HYSPLIT model

Atmospheric transport during the 2014 SOAS field study was analyzed by computing air trajectories using the HYSPLIT Model (<http://ready.arl.noaa.gov/HYSPLIT.php>) from the Air Resources Laboratory of the National Oceanic and Atmospheric Administration (NOAA). Wind fields from the NOAA-NCAR Global Reanalysis data set were used as input to HYSPLIT for trajectory calculations. Vertical air parcel motion was determined from estimated vertical velocities in the input data set. Air trajectories were computed 24 hours backward in time from Look Rock in one-hour time steps with ending heights at Look Rock of 100, 500 and 1500 m above ground level. Each trajectory arrived at Look Rock at midnight (EST) or 01:00 EDT.

To further examine the influence of NO_x emissions as well as aerosol acidity, we examined where air masses originated from to our site using back trajectory (HYSPLIT model) analysis. Figs. S12 and S13 present the back-trajectories of air mass arrived at the LRK site at 01:00 local time (00:00 EST) of the date on each plot. During periods (10 – 16 June 2013) of high levels of IEPOX-derived SOA mass, the model shows that air masses were coming from the south at the beginning and slowly shifted from the west for the next three days (Fig. S12). Throughout periods when IEPOX-derived SOA is low (2 – 8 July 2013), air masses were coming from the south and southeast. Considering that the site is located at about 800 m above sea level, it is less likely that the air masses (at 100 m above the surface) carried NO_x from nearby sources. Air masses at 500 m and 1500 m above the surface might carry some NO_x, however, it might have been diluted during the transport.



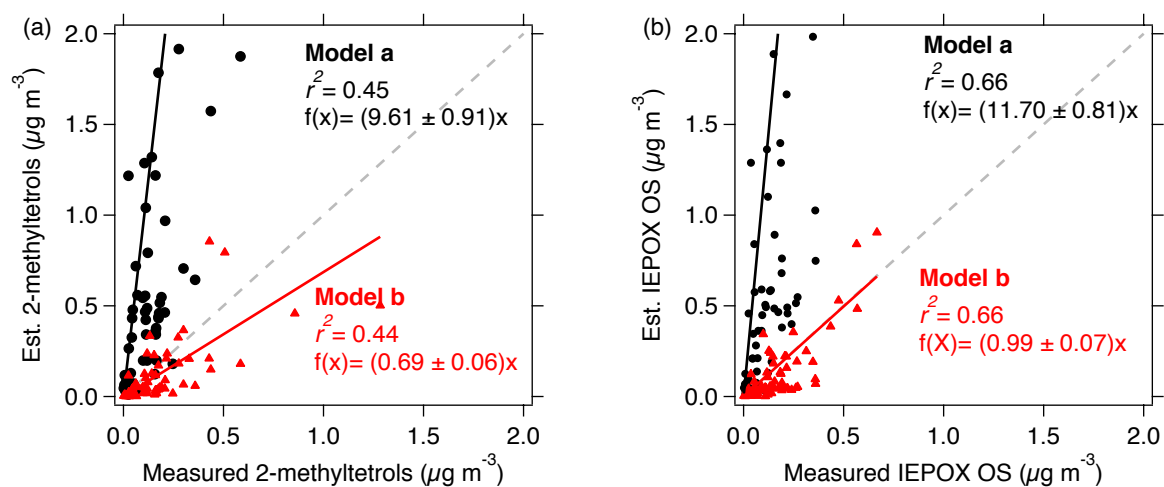
1 **Figure S12.** Air mass back trajectories from HYSPLIT 24-hr model during the first and
2 second intensive filter sampling periods when high IEPOX-derived SOA formation was
3 observed. The backtrajectories were estimated at elevation of 100 m (orange), 500 m
4 (turquoise), and 1500 m (purple) above the site. Concentration of IEPOX-derived SOA started
5 to decrease on June 17, 2013.



1 **Figure S13.** Air mass back trajectories from HYSPLIT 24-hr model during low IEPOX-
2 derived SOA formation of 2 – 8 July 2013. 9 July 2013 was the beginning of the fourth
3 intensive period. The backtrajectories were estimated at elevation of 100 m (orange), 500 m
4 (turquoise), and 1500 m (purple) above the site.

1 Results from simpleGAMMA

2



3 **Figure S14.** Correlation of (a) 2-methyltetrols and (b) IEPOX-derived organosulfate (IEPOX
 4 OS) estimated by simpleGAMMA by assuming H^* of 3.0×10^7 (Nguyen et al., 2014)
 5 (model a) and 2.7×10^6 (Pye et al., 2013) (model b).

6